JOURNAL OF AIRCRAFT
Vol. 45, No. 3, May–June 2008

Thermoacoustic Random Response of Shape Memory Alloy Hybrid Composite Plates

Hesham H. Ibrahim*
National Authority for Remote Sensing and Space Sciences, Cairo 11769, Egypt
Mohammad Tawfik†
British University in Egypt, Cairo 11837, Egypt
and
Hani M. Negm‡
Cairo University, Cairo 12613, Egypt

DOI: 10.2514/1.32843

Random dynamic response and thermal buckling of a shape memory alloy hybrid composite plate subjected to combined thermal and random acoustic loads are investigated. A nonlinear finite element model was developed using the first-order shear-deformable plate theory, von Kármán strain-displacement relations, and the principle of virtual work. The thermal load was assumed to be a steady-state constant-temperature distribution, whereas the acoustic excitation was modeled as a white-Gaussian pressure with zero mean and uniform magnitude over the plate surface. To account for the nonlinear temperature dependence of material properties, the thermal strain was stated as an integral quantity of the thermal expansion coefficient with respect to temperature. The static nonlinear equations of motion are solved by the Newton–Raphson iteration technique to obtain the thermal postbuckling deflection, whereas the dynamic nonlinear equations of motion were transformed to modal coordinates and solved by employing Newmark implicit integration scheme. Finally, the critical buckling temperatures, static thermal postbuckling deflections, and random dynamic responses of a shape memory alloy hybrid-composite-plate panel are presented, illustrating the effect of shape memory alloy fiber embedding, sound pressure level, and temperature rise on the panel response.

I. Introduction

THE external skin of high-speed flight vehicles experience high temperatures due to aerodynamic heating, which can induce thermal buckling and may result in a dynamic instability. In general, thermal buckling does not indicate structural failure. However, large thermal deflections of the skin panel can change its aerodynamic shape, causing reduction in the flight performance.

A comprehensive literature review on thermally induced flexure, buckling, and vibration of plates and shells was presented by Tauchart [1] and Thornton [2]. Gray and Mei [3] investigated the thermal postbuckling behavior and free vibration of thermally buckled composite plates using the finite element method. Shi et al. [4] adopted a finite element modal method to solve the problem of thermal postbuckling of composite plates with initial imperfections. Jones and Mazumdar [5] investigated the linear and nonlinear dynamic behavior of plates at elevated temperatures. They presented analytical solutions for the thermal buckling and postbuckling behavior of a plate strip. Shi et al. [6] presented a finite element solution for the thermal buckling behavior of laminated composite plates under combined mechanical and thermal loads. Ibrahim et al. [7] investigated the thermal buckling and flutter boundaries of thin functionally graded material plates at elevated temperature. They adopted an incremental finite element technique to capture the effect of the temperature dependence of material properties on the panel response. Ibrahim et al. [8] presented a finite element solution for the thermal buckling and nonlinear flutter performance of thin functionally graded material panels under combined aerodynamic and thermal loads. To account for the temperature dependence of material properties, the thermal strain was modeled as an integral quantity of thermal expansion coefficient with respect to temperature. Ibrahim et al. [9] extended the formulation presented in [8] by including the shear deformation effect to make it capable of handling thick functionally graded material plates.

The surface panels of advanced high-speed aircraft and spacecraft may exhibit large random vibration under high acoustic loads and may possibly experience both random vibration and thermal buckling at elevated temperatures. Both of these effects are nonlinear in nature and make the prediction of fatigue life extremely difficult. A literature review on the nonlinear response and sonic fatigue of surface panels was presented by Vaicaitis [10]. Experiments to study thermally loaded panels under random excitation were performed by Istenes et al. [11], Ng and Clevenson [12], and Murphy et al. [13] in which a snap-through phenomenon and frequency shifting due to nonlinear large-amplitude vibration were observed. Kavallieratos and Vaicaitis [14] studied the nonlinear response of composite skin panels of high-speed aircraft. Locke [15] investigated the large deflection random vibration of a thermally buckled thin isotropic plate using the method of equivalent linearization and assuming temperature-independent material properties. Abdel-Motagaly et al. [16] adopted finite element numerical integration to study the nonlinear panel response of thick composite-plate panels under combined aerodynamic and acoustic loads. Dhainaut et al. [17,18] presented a finite element solution for the prediction of nonlinear random response of thin isotropic and composite panels subjected to the simultaneous action of band-limited white-Gaussian noise and elevated temperatures. Dhainaut and Mei [19] investigated the nonlinear response and fatigue-life estimation of thin isotropic panels subjected to nonwhite acoustic excitation. Results showed that the actual flight data with nonwhite power spectral density can yield higher stress characteristics and shorter fatigue life than those of the corresponding equivalent white noise. Ibrahim et al. [20] studied the nonlinear random vibration of thin, temperature-dependent, functionally graded material plate panels under

Received 16 June 2007; revision received 6 November 2007; accepted for publication 18 December 2007.

*Assistant Professor, Space Division; hesham.ibrahim@narss.sci.eg.
†Mechanical Engineering Department; Mohammad.tawfik@bue.edu.eg.
‡Professor, Aerospace Engineering Department, Faculty of Engineering; Hmnegm_cu@hotmail.com.

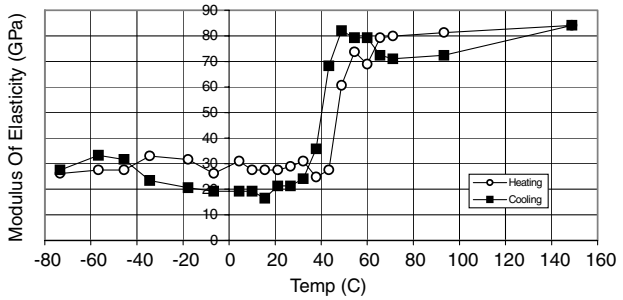

Fig. 1 Variation of the SMA modulus of elasticity with temperature.

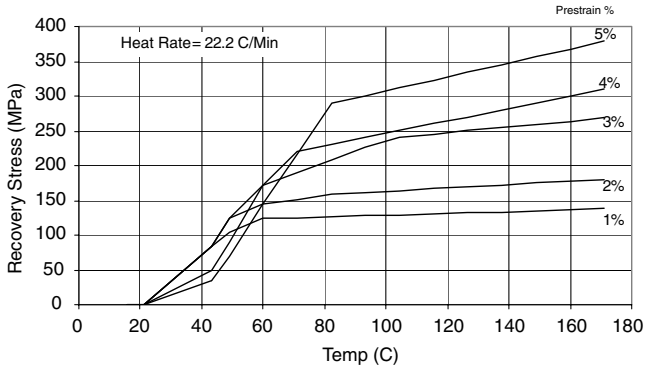

Fig. 2 Constrained shape-recovery stresses of the SMA fibers as a function of temperature and prestrain value.

combined random acoustic and thermal loads. It was found that decreasing the postbuckling deflection through increasing the ceramic volume fraction enhances the domination of the acoustic random vibration over the thermal buckling deflection, which might not be favorable regarding the fatigue-life performance of the plate.

Shape memory alloys (SMAs) have a unique ability to completely recover large prestrains (up to 10% elongation) when heated above a certain characteristic temperature. During the shape-recovery process, a large tensile recovery stress occurs if the SMA is restrained. Both the recovery stresses and Young's modules of SMAs exhibit nonlinear temperature-dependent properties, as shown in Figs. 1 and 2 [21].

Birman [22] presented a comprehensive review on the literature concerning SMAs up to 1997. Jia and Rogers [23] formulated a mechanical model for composite plates with embedded shape memory alloy fibers using the micromechanical behavior of the highly nonlinear shape memory alloy. Tawfik et al. [24] proposed a novel concept of enhancing the thermal buckling and aeroelastic behavior of plates through embedding SMA fibers in them. They adopted an incremental technique to account for the temperature dependence of material properties. Park et al. [25] presented an incremental finite element solution for the nonlinear vibration behavior of thick thermally buckled composite plates embedded with shape memory alloy fibers. Gilat and Aboudi [26] derived micromechanically established constitutive equations for unidirectional composites with shape memory alloy fibers embedded in polymeric metallic matrices. Those equations were subsequently employed to analyze the nonlinear behavior of infinitely wide composite plates that are subject to sudden application of thermal loading. Gou et al. [27] developed an efficient finite element procedure to predict large-amplitude nonlinear random response of thin SMA hybrid composite (SMAHC) plates subject to combined thermal and acoustic excitations. Ibrahim et al. [28] investigated the thermal buckling of thick SMAHC plates. Moreover, a frequency domain solution for predicting panel flutter boundaries at elevated temperatures was presented.

This paper is an extension of the work presented in [27] by including the shear deformation effect in the mathematical model to make it capable of handling thick plates. In this work, a new nonlinear finite element model is presented for modeling the thermal buckling and nonlinear random dynamic behavior of thick SMAHC plate panels under the combined effect of thermal and random acoustic loads. The governing equations of motion are obtained using the first-order shear-deformable plate theory, von Kármán strain-displacement relations, and the principle of virtual work. To account for the nonlinear temperature dependence of material properties, the thermal strain is modeled as an integral quantity of the thermal expansion coefficient with respect to temperature. Therefore, the method does not need the use of many small temperature increments as in the incremental method presented in [24]. Numerical results are provided to show the effect of the prestrained SMA fiber embedding on the thermal buckling and the nonlinear random dynamic response of a traditional composite-plate panel with different boundary conditions.

II. Finite Element Formulation

A. Nonlinear Strain-Displacement Relations

The nodal degrees of freedom vector of a nine-noded rectangular plate element can be written as

$$\{w\} = \{\{w_b\}, \{\phi_x, \phi_y\}, \{u, v\}\}^T = \begin{Bmatrix} \{w_b\} \\ \{w_\phi\} \\ \{w_m\} \end{Bmatrix} = \begin{Bmatrix} \{w_B\} \\ \{w_m\} \end{Bmatrix} \tag{1}$$

where $\{w_b\}$ is the transverse displacement vector of the middle plane; ϕ_x and ϕ_y are rotations of the transverse normal about the x and y axes; and u and v are the membrane displacements in the x and y directions. In-plane strains and curvatures, based on von Kármán's moderately large deflection and the first-order shear-deformable plate theory, are given by [29]

$$\begin{Bmatrix} \varepsilon_x \\ \varepsilon_y \\ \gamma_{xy} \end{Bmatrix} = \begin{Bmatrix} \frac{\partial u}{\partial x} \\ \frac{\partial v}{\partial y} \\ \frac{\partial u}{\partial y} + \frac{\partial v}{\partial x} \end{Bmatrix} + \begin{Bmatrix} \frac{1}{2}\left(\frac{\partial w}{\partial x}\right)^2 \\ \frac{1}{2}\left(\frac{\partial w}{\partial y}\right)^2 \\ \frac{\partial w}{\partial x}\frac{\partial w}{\partial y} \end{Bmatrix} + z \begin{Bmatrix} \frac{\partial \phi_y}{\partial x} \\ \frac{\partial \phi_x}{\partial y} \\ \frac{\partial \phi_y}{\partial y} + \frac{\partial \phi_x}{\partial x} \end{Bmatrix}$$

$$= \{\varepsilon_{\text{lin}}\} + \{\varepsilon_\theta\} + z\{\kappa\} \tag{2}$$

where ε_{lin}, ε_θ, and $z\{\kappa\}$ are the membrane linear strain vector, the membrane nonlinear strain vector, and the bending strain vector, respectively. In addition, the transverse shear strain vector can be expressed as [29]

$$\begin{Bmatrix} \gamma_{yz} \\ \gamma_{xz} \end{Bmatrix} = \begin{Bmatrix} \phi_x \\ \phi_y \end{Bmatrix} + \begin{Bmatrix} \frac{\partial w}{\partial y} \\ \frac{\partial w}{\partial x} \end{Bmatrix} \tag{3}$$

B. Constitutive Equations

For the kth composite lamina impregnated with SMA fibers, the stress-strain relations can be expressed as [27]

$$\{\sigma\}^k = \begin{Bmatrix} \sigma_x \\ \sigma_y \\ \tau_{xy} \end{Bmatrix}^k$$

$$= [\bar{Q}(T)]^k\{\varepsilon\} + \{\sigma_r(T)\}^k V_s^k - [\bar{Q}(T)]_m^k V_m^k \int_{T_{\text{ref}}}^{T} \{\alpha(\tau)_m^k\}\, \mathrm{d}\tau \tag{4}$$

$$\{\tau\}^k = \begin{Bmatrix} \tau_{yz} \\ \tau_{xz} \end{Bmatrix}^k = \begin{bmatrix} \bar{Q}_{44}(T) & \bar{Q}_{45}(T) \\ \bar{Q}_{45}(T) & \bar{Q}_{55}(T) \end{bmatrix} \begin{Bmatrix} \gamma_{yz} \\ \gamma_{xz} \end{Bmatrix} \tag{5}$$

where $\{\sigma\}$, $\{\sigma_r\}$, and $\{\tau\}$ are the in-plane stress vector, the SMA recovery-stress vector at a given temperature T, and the transverse shear stress vector, respectively; V_m and V_s are the volume fractions of the composite matrix and SMA fibers, respectively; and $\{\alpha\}_m$, $[\bar{Q}]$, and $[\bar{Q}]_m$ are the thermal expansion coefficient vector of the

composite matrix, the transformed reduced stiffness matrix of the SMA embedded lamina, and the transformed reduced stiffness matrix of the composite matrix, respectively. Note that the SMA fiber is embedded in same direction of the composite matrix fibers and is assumed to be uniformly distributed within each layer. Integrating Eqs. (4) and (5) over the plate thickness h, the constitutive equation is obtained as

$$\begin{Bmatrix}\{N\}\\ \{M\}\end{Bmatrix}=\begin{bmatrix}[A] & [B]\\ [B] & [D]\end{bmatrix}\begin{Bmatrix}\{\varepsilon_{\text{lin}}\}+\{\varepsilon_\theta\}\\ \{\kappa\}\end{Bmatrix}-\begin{Bmatrix}\{N^T\}\\ \{M^T\}\end{Bmatrix}+\begin{Bmatrix}\{N_r\}\\ \{M_r\}\end{Bmatrix} \quad (6)$$

$$\{R\}=\begin{Bmatrix}R_{yz}\\ R_{xz}\end{Bmatrix}=\begin{bmatrix}A_{44} & A_{45}\\ A_{45} & A_{55}\end{bmatrix}\begin{Bmatrix}\gamma_{yz}\\ \gamma_{xz}\end{Bmatrix}=[A]^s\{\gamma\} \quad (7)$$

where

$$(\{N^T\},\{M^T\})=\int_{-h/2}^{h/2}\left[[Q(T)]\left(\int_{T_{\text{ref}}}^{T}\alpha(\tau)\,\mathrm{d}\tau\right)\right](1,z)\,\mathrm{d}z$$

$$(\{N_r\},\{M_r\})=\int_{-h/2}^{h/2}\{\sigma_r\}V_s(1,z)\,\mathrm{d}z$$

C. Governing Equations

By using the principle of virtual work and Eqs. (2), (3), (6), and (7), the nonlinear governing equation can be derived as follows:

$$\delta\text{work}=\delta\text{work}_{\text{int}}-\delta\text{work}_{\text{ext}}=0 \quad (8)$$

The internal virtual work $\delta\text{work}_{\text{int}}$ can be stated as

$$\begin{aligned}\delta\text{work}_{\text{int}}&=\int_A(\{\delta\varepsilon_m\}^T\{N\}+\{\delta\kappa\}^t\{M\}+K\{\delta\gamma\}^T\{R\})\,\mathrm{d}A\\&=\{\delta w\}^T\left([k]-[k_T]+[k_r]+\frac{1}{2}[n1]+\frac{1}{3}[n2]\right)\{w\}\\&\quad-\{\delta w\}^T(\{p_T\}-\{p_r\})\end{aligned} \quad (9)$$

where $[k]$, $[k_T]$, and $[k_r]$ are the linear, thermal, and recovery-stress stiffness matrices; $[n1]$ and $[n2]$ are the first- and second-order nonlinear stiffness matrices; K is a shear correction factor; and $\{p_T\}$ and $\{p_r\}$ are the thermal and recovery-stress vectors. The external virtual work $\delta\text{work}_{\text{ext}}$ can be stated as

$$\begin{aligned}\delta\text{work}_{\text{ext}}&=\int_A(-I_o(\{\delta u\}^T\{\ddot{u}\}+\{\delta v\}^T\{\ddot{v}\}+\{\delta w\}^T\{\ddot{w}_b\})\\&\quad-I_2(\{\delta\phi_x\}^T\{\ddot{\phi}_x\}+\{\delta\phi_y\}^T\{\ddot{\phi}_y\})+\{\delta w_b\}^T p(t))\,\mathrm{d}A\\&=-\{\delta w\}^T[m]\{\ddot{w}\}+\{\delta w_b\}^T P(t)\end{aligned} \quad (10)$$

where

$$(I_o,I_2)=\int_{-h/2}^{h/2}\rho(1,z^2)\,\mathrm{d}z$$

$[m]$ is the mass matrix, and $p(t)$ is the acoustic load modeled as a white-Gaussian pressure. By substituting Eqs. (9) and (10) into Eq. (8), the governing equations for a SMAHC plate under the combined action of thermal and random acoustic loads can be stated as

$$\begin{aligned}&\begin{bmatrix}M_B & 0\\ 0 & 0\end{bmatrix}\begin{Bmatrix}\ddot{W}_B\\ \ddot{W}_m\end{Bmatrix}+\left(\begin{bmatrix}K_B & 0\\ 0 & K_m\end{bmatrix}-\begin{bmatrix}K_{TB} & 0\\ 0 & 0\end{bmatrix}+\begin{bmatrix}K_{rB} & 0\\ 0 & 0\end{bmatrix}\right.\\&\left.+\frac{1}{2}\begin{bmatrix}N1_{NmB} & N1_{Bm}\\ N1_{mB} & 0\end{bmatrix}+\frac{1}{3}\begin{bmatrix}N2_B & 0\\ 0 & 0\end{bmatrix}\right)\begin{Bmatrix}W_B\\ W_m\end{Bmatrix}\\&=\begin{Bmatrix}P_B(t)\\ 0\end{Bmatrix}+\begin{Bmatrix}0\\ P_{mT}\end{Bmatrix}-\begin{Bmatrix}0\\ P_{mr}\end{Bmatrix}=\begin{Bmatrix}P_B\\ P_m\end{Bmatrix}\end{aligned} \quad (11)$$

or, in a more compact form, as

$$\begin{aligned}&[M]\{\ddot{W}\}+([K]-[K_T]+[K_r]+\tfrac{1}{2}[N1]+\tfrac{1}{3}[N2])\{W\}\\&\quad=\{P(t)\}+\{P_T\}-\{P_r\}\end{aligned} \quad (12)$$

Note that neglecting the in-plane inertia terms in Eq. (11) will not bring significant error, because their natural frequencies are usually two to three orders of magnitude higher than those of bending [16].

III. Solution Procedures

A. Static Thermal Buckling

For the static thermal buckling problem, Eq. (12) reduces to

$$\left([K]-[K_T]+[K_r]+\tfrac{1}{2}[N1]+\tfrac{1}{3}[N2]\right)\{W\}=\{P_T\}-\{P_r\} \quad (13)$$

Introducing the function $\{\Psi(W)\}$ to Eq. (13),

$$\begin{aligned}\{\Psi(W)\}&=\left([K]-[K_T]+[K_r]+\tfrac{1}{2}[N1]+\tfrac{1}{3}[N2]\right)\{W\}\\&\quad-\{P_T\}+\{P_r\}=0\end{aligned} \quad (14)$$

Equation (14) can be written in the form of a truncated Taylor series expansion as

$$\{\Psi(W+\delta W)\}=\{\Psi(W)\}+\frac{\mathrm{d}\{\Psi(W)\}}{\mathrm{d}(W)}\{\delta W\}\cong 0 \quad (15)$$

where [24]

$$\frac{\mathrm{d}\{\Psi(W)\}}{\mathrm{d}(W)}=([K]-[K_T]+[K_r]+[N1]+[N2])=[K_{\tan}] \quad (16)$$

Thus, the Newton–Raphson iteration procedure for the determination of the thermal postbuckling deflection can be expressed as follows:

$$\begin{aligned}\{\Psi(W)\}_i&=\left([K]-[K_T]+[K_r]+\tfrac{1}{2}([N1])_i+\tfrac{1}{3}([N2])_i\right)\{W\}\\&\quad-\{P_T\}+\{P_r\}\\[K_{\tan}]_i\{\delta W\}_{i+1}&=-\{\Psi(W)\}_i\\\{\delta W\}_{i+1}&=-[K_{\tan}]^{-1}\{\Psi(W)\}_i\\\{W\}_{i+1}&=\{W\}_i+\{\delta W\}_{i+1}\end{aligned}$$

Convergence occurs in the preceding procedure when the maximum value of $\{\delta W\}_{i+1}$ becomes less than a given tolerance ε_{tol} (i.e., $\max|\{\delta W\}_{i+1}|\le\varepsilon_{\text{tol}}$).

B. Nonlinear Thermoacoustic Response Using Modal Transformation

In this section, a time-domain solution is presented for the nonlinear dynamic response of symmetrically laminated SMAHC plates. Separating the membrane and transverse displacement equations in Eq. (11) results in

$$[M_B]\{\ddot{W}_B\} + \left([K_B] - [K_{TB}] + [K_{rB}] + \tfrac{1}{2}[N1_{NmB}(\{W_m\})] + \tfrac{1}{3}[N2_B]\right) \times \{W_B\} + \tfrac{1}{2}[N1_{Bm}]\{W_m\} = \{P_B\} \quad (17)$$

$$[K_m]\{W_m\} + \tfrac{1}{2}[N1_{mB}]\{W_B\} = \{P_m\} \quad (18)$$

From Eq. (18), the in-plane displacement vector $\{W_m\}$ can be expressed in terms of the bending displacement vector $\{W_B\}$ as

$$\{W_m\} = [K_m]^{-1}\{P_m\} - \tfrac{1}{2}[K_m]^{-1}[N1_{mB}]\{W_B\} = \{W_m\}_o - \{W_m\}_2 \quad (19)$$

Substituting Eq. (19) into Eq. (17), the system equations of motion can be finally expressed as a function of $\{W_B\}$ as [30]

$$[M_B]\{\ddot{W}_B\} + ([K_B] - [K_{TB}] + [K_{rB}] + [N1_{NmB}(\{W_m\}_o)])\{W_B\} + (\tfrac{1}{3}[N2_B] - \tfrac{1}{2}[N1_{NmB}(\{W_m\}_2)] - \tfrac{1}{4}[N1_{Bm}][K_m]^{-1}[N1_{mB}])\{W_B\} = \{P_B\} \quad (20)$$

Equation (20) can be numerically integrated in the structural nodal degrees of freedom. But this approach turns out to be computationally expensive. Therefore, an alternative and effective solution procedure is to transform Eq. (20) into modal coordinates using reduced system normal modes by expressing the system bending displacement $\{W_B\}$ as a linear combination of a finite number of normal mode shapes as

$$\{W_B\} \approx \sum_{r=1}^{n} q_r\{\phi_r\} = [\Phi]\{q\} \quad (21)$$

where the rth normal mode $\{\phi_r\}$ and the corresponding natural frequency ω_r are obtained from the linear vibration of the system as

$$\omega_r^2[M_B]\{\phi_r\} = ([K_B])\{\phi_r\} \quad (22)$$

Accordingly, all the matrices in Eq. (20) are transformed into modal coordinates and Eq. (20) can be written in modal coordinates as

$$[\bar{M}_B]\{\ddot{q}\} + 2[\zeta_r f_r][\bar{M}_B]\{\dot{q}\} + ([\bar{K}] + [\bar{K}_{qq}])\{q\} = \{\bar{P}_B\} \quad (23)$$

Note that a modal structural damping matrix $2[\zeta_r f_r][M_B]$ was added to Eq. (23) to account for the structural damping effect on the system [27]. The coefficient ζ_r is the modal damping ratio of the rth mode, and f_r is the rth natural frequency in hertz.

IV. Numerical Results and Discussions

Numerical analyses for the thermal buckling and the nonlinear acoustic random vibration of a laminated composite-plate panel with and without SMA fibers are performed using the finite element method. The plate dimensions are chosen to be $0.381 \times 0.305 \times 0.0013$ m and the stacking sequence is $[0/-45/45/90]_s$. A uniform 6×6 finite element mesh gives a converged solution and is thus used. A reduced-order numerical integration is used for the terms related to the transverse shear to avoid shear locking. In addition, 5, 10, and 15% volume fractions and 1, 3, and 5% initial prestrain values of the SMA fibers are used.

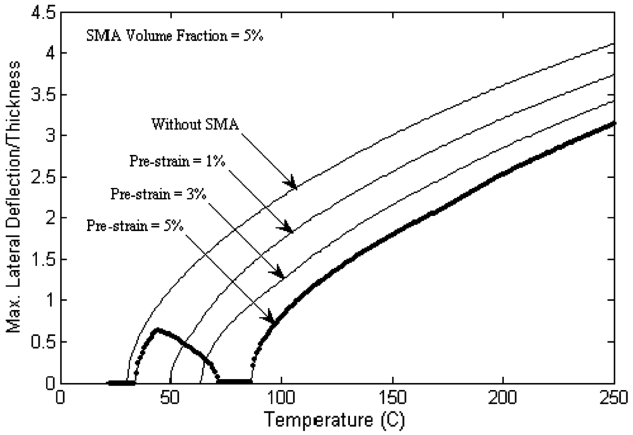

Fig. 3 Maximum nondimensional postbuckling deflections for a simply supported SMAHC plate with 5% volume fraction and different prestrain values.

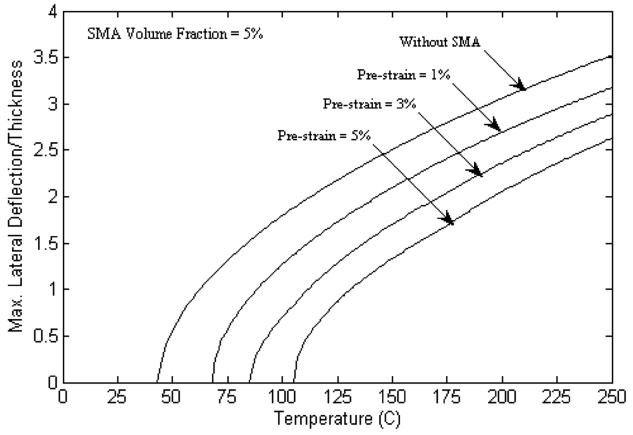

Fig. 4 Maximum nondimensional postbuckling deflections for a clamped SMAHC plate with 5% volume fraction and different prestrain values.

A. Thermal Buckling Analysis

The thermal postbuckling behavior of a traditional laminated composite plate with and without SMA is studied. Clamped and simply supported boundary conditions are studied. Table 1 presents the material properties of the composite matrix and SMA fibers [28]. A uniform temperature elevation is applied to the plate, and the reference temperature is assumed to be 21°C.

Figures 3 and 4 present the postbuckling deflection for three different prestrains of SMA fibers with 5% volume fraction. Comparing the buckling temperatures of the SMAHC plate with that of a composite plate with the same in-plane dimensions and weight, it is found that the buckling temperature for a simply supported SMAHC plate, seen in Fig. 3, is increased by 143, 317, and 465% for

Table 1 Material properties of the composite matrix and SMA fiber

Nitinol	Graphite-epoxy
See Figs. 1 and 2 for Young's modulus and recovery stresses.	E1 $155(1 - 6.35 \times 10^{-4}\Delta T)$ GPa
	E2 $8.07(1 - 7.69 \times 10^{-4}\Delta T)$ GPa
G 25.6 GPa	G12 $4.55(1 - 1.09 \times 10^{-3}\Delta T)$ GPa
ρ 6450 kg/m^3	ρ 1550 kg/m^3
ν 0.3	ν 0.22
α 10.26×10^{-6}/°C	$\alpha 1$ $-0.07 \times 10^{-6}(1 - 0.69 \times 10^{-3})\Delta T$/°C
	$\alpha 2$ $30.6 \times 10^{-6}(1 + 0.28 \times 10^{-4})\Delta T$/°C

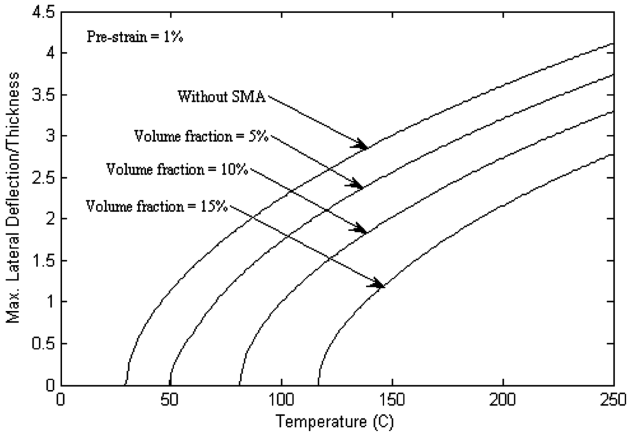

Fig. 5 Maximum nondimensional postbuckling deflections for a simply supported SMAHC plate with 1% prestrain and different volume fractions.

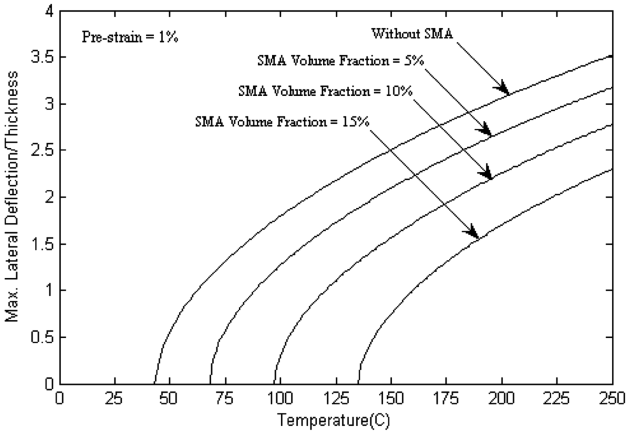

Fig. 6 Maximum nondimensional postbuckling deflections for a clamped SMAHC plate with 1% prestrain and different volume fractions.

1, 3, and 5% prestrains, respectively. It is also seen that the 5%-prestrain case has two buckling temperatures. This is because the 5%-prestrain curve for the temperature range from 21 to 43°C, shown in Fig. 2, has a slower rate of recovery-stress increase with temperature than that of the 1 and 3% prestrains, which makes the thermal stress dominate the SMA recovery stress during this temperature range and hence the plate experiences thermal buckling. But for temperatures above 43°C, the 5%-prestrain curve has a higher rate of increase than that of temperatures lower than 43°C, which causes the recovery stress to dominate the thermal stress to make the plate go flat again at 72°C before reaching the second thermal buckling point at 86°C. That is why the performance of the 5% prestrain is always lower than that of the 1 and 3% values in the temperature range from 21 to 43°C (i.e., from room temperature up to a temperature increase of 22°C). For the clamped SMAHC plate, seen in Fig. 4, it is found that its buckling temperatures are increased by 54, 109, and 175% for 1, 3, and 5% prestrains, respectively, compared with those of a composite plate with equivalent weight.

Figures 5 and 6 demonstrate the impact of changing the SMA volume fraction on the critical bucking temperature and the postbuckling deflection for both simply supported and clamped SMAHC plates. It is seen that increasing the volume of SMA improves the thermal stability of SMAHC plates for both plate boundary conditions.

B. Panel Response Under Combined Thermal and Random Acoustic Loads

The plate nonlinear random vibration behavior is investigated with two parameters in the study: temperature rise ΔT and sound pressure level SPL, where ΔT varies from 0–150°C, and SPL varies from 90–130 dB. A traditional clamped composite plate and a SMAHC plate with 5% volume fraction and 3% prestrain are studied and compared. A proportional damping ratio of $\zeta_r f_r = \zeta_s f_s$ is used with a fundamental modal damping coefficient ζ_1 equal to 0.02 [27]. The Newmark implicit numerical integration scheme is used to solve the system differential equations with a time step of 1/10,000 s [31], and the Newton–Raphson iteration scheme is adopted to solve the nonlinear algebraic system of equations at each time step. Six normal modes give a converged root mean square (rms) deflection and are thus used. To eliminate the effect of initial transient response, the first 0.1 s out of a total period of 1-s time history is excluded from the statistical process.

Figure 7 presents the time-history response of a clamped traditional composite plate at SPL = 90 dB and temperature rises of 0, 50, 100, and 150°C. It can be seen that at room temperature, the plate exhibits basically small-deflection (rms=0.0744) random vibration. At temperature rises of 50, 100, and 150°C, which are beyond the critical buckling temperature of the plate ($\Delta T_{cr} = 22.5$°C), the plate experiences small random vibration

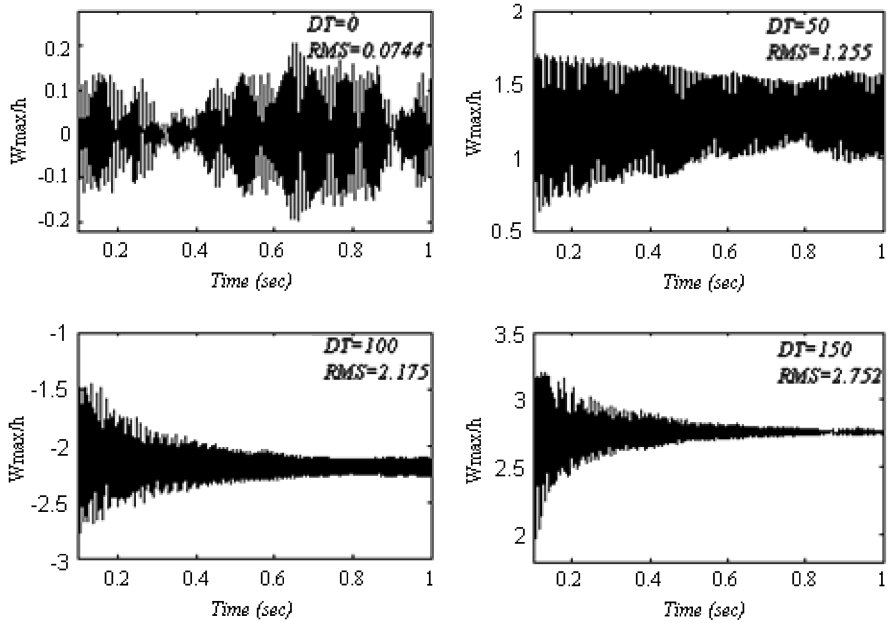

Fig. 7 Random vibration response of a clamped traditional composite plate at SPL = 90 dB and various temperature rises ΔT.

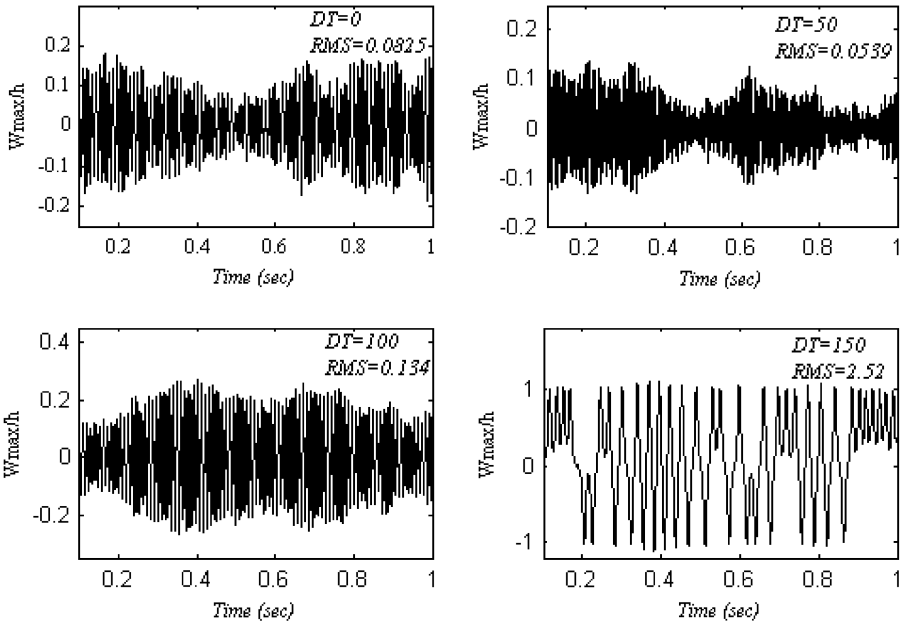

Fig. 8 Random vibration response of a clamped SMAHC plate at SPL = 90 dB and various temperature rises ΔT.

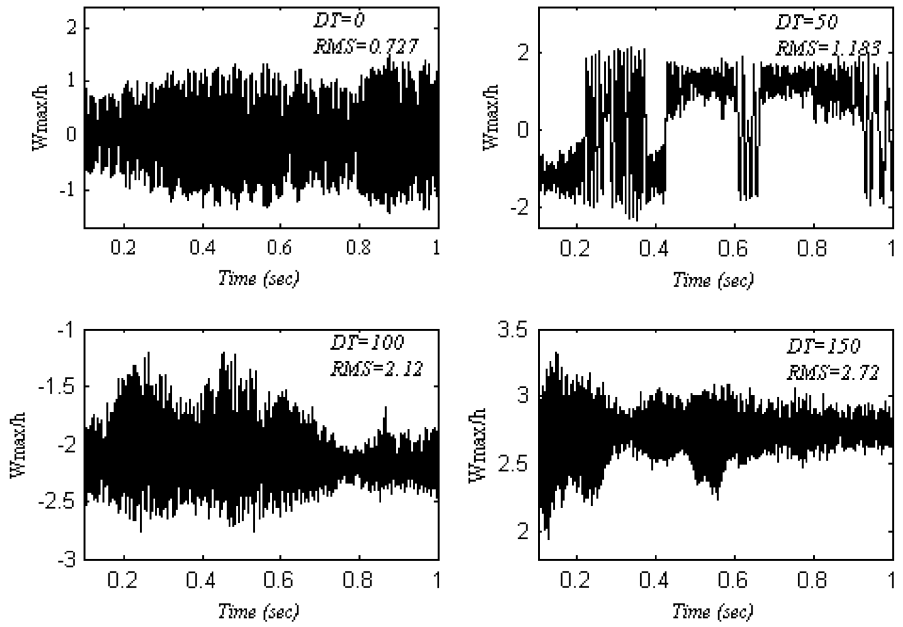

Fig. 9 Random vibration response of a clamped traditional composite plate at SPL = 110 dB and various temperature rises ΔT.

about the static postbuckling deflections $W_{\max}/h$ of 1.22, −2.12, and 2.72, respectively. It is also noticed that the vibration amplitude decreases as temperature increases beyond $\Delta T_{\rm cr}$, because nonlinear stiffness terms add stiffness to the plate as thermal deflection increases.

Figure 8 presents the time-history response of a clamped SMAHC plate at SPL = 90 dB and temperature rises of 0, 50, 100, and 150°C. It is seen that at room temperature, the plate randomly vibrates with a small deflection rms = 0.0825, which is slightly higher than that of the traditional composite plate, due to the higher weight of the SMAHC plate and the SMA fibers not being activated yet. At a temperature rise of 50°C, the activation of SMA fibers results in a lower vibration amplitudes and deflection rms values than that of the traditional composite plate presented in Fig. 7. At a temperature rise of 100°C, the thermal compressive stress dominates the SMA recovery stress results in higher vibration amplitudes and deflection rms values than those with the 0 and 50°C temperature rises. At a temperature rise of 150°C, which is beyond the critical buckling temperature of the SMAHC plate ($\Delta T_{\rm cr} = 136$°C), it is seen that the plate experiences a persistent snap-through motion that covers both thermal buckling equilibrium positions, because the nonlinear stiffness has not yet compensated the critically lowered stiffness due to temperature rise.

Figure 9 presents the time-history response of a clamped traditional composite plate at SPL = 110 dB. It is seen that at room temperature, the plate randomly vibrates with deflection rms = 0.725, which is much higher than that of the 90 dB case. At a temperature rise of 50°C, the plate shows very clear snap-through between the two buckling equilibrium positions (±1.22). At temperature rises of 100 and 150°C, the occurrence of snap-through is resisted by the stiffness added by the increased thermal postbuckling deflection, resulting in completely hindering snap-

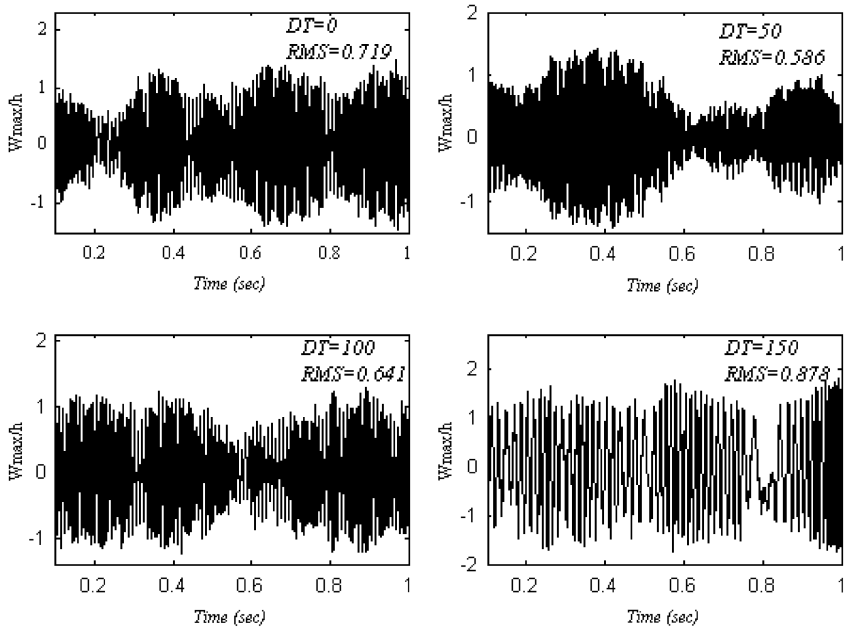

Fig. 10 Random vibration response of a clamped SMAHC plate at SPL = 110 dB and various temperature rises ΔT.

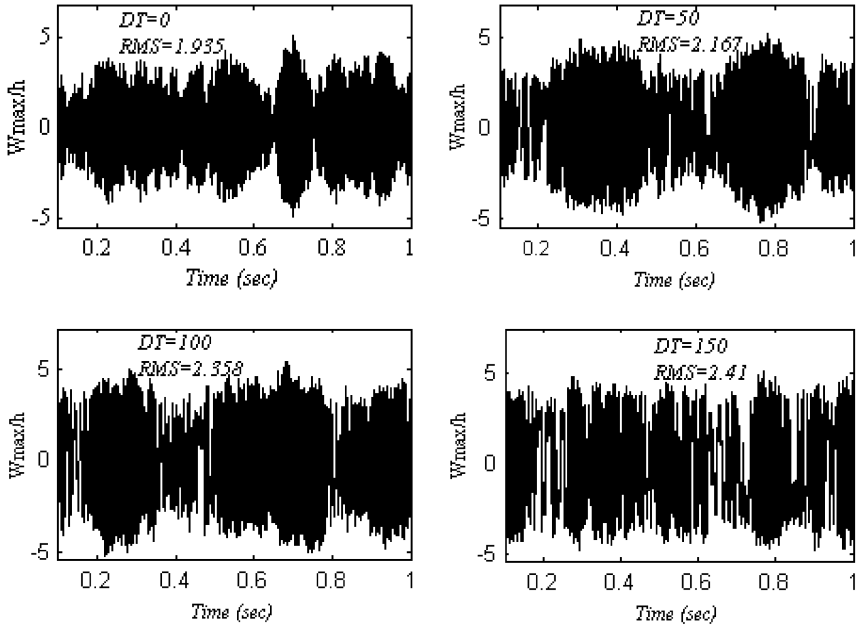

Fig. 11 Random vibration response of a clamped traditional composite plate at SPL = 130 dB and various temperature rises ΔT.

through motions, and the plate shows moderate-deflection rms random vibration about the buckling equilibrium positions $W_{\max}/h = -2.12$ and 2.72.

For the clamped SMAHC plate, presented in Fig. 10, it is seen that the plate exhibits moderate-deflection random vibration for the temperature rises of 0, 50, and 100°C. At a temperature rise of 150°C, it is seen that the plate experiences a persistent snap-through that covers both buckling equilibrium positions. It is also observed that the plate has a lower rms deflection at 50°C temperature rise than that at 100°C, because the recovery stress dominates the thermal expansion in the vicinity of the 50°C temperature rise.

For the case of a 130-dB sound pressure level at different values of temperature rise, shown in Figs. 11 and 12, both traditional composite and SMAHC plates show large-amplitude nonlinear random vibrations. It is also found that the SMA fiber embedding has no pronounced effect on the panel response, because the acoustic pressure completely dominates the thermal and the constrained shape-recovery stresses.

V. Conclusions

A traditional composite plate impregnated with prestrained shape memory alloy fibers and subjected to the combined effect of thermal and random acoustic loads was studied. A nonlinear finite element model based on the first-order shear-deformable plate theory was adopted to study the effect of using SMA fiber embedding on the static and dynamic response of composite plates. The nonlinear temperature dependence of material properties was considered in the formulation. Newton–Raphson iteration was employed to obtain the static thermal deflection at each temperature step, and the dynamic response at each time step of the Newmark numerical integration

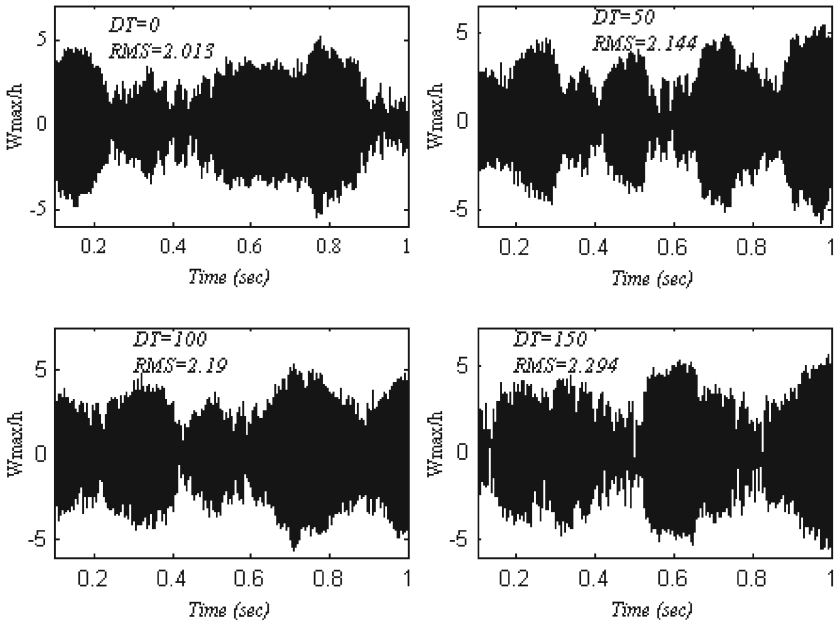

Fig. 12 Random vibration response of a clamped SMAHC plate at SPL = 130 dB and various temperature rises ΔT.

scheme. Finite element modal formulation and solution procedures are developed for the time-domain method.

Results showed that SMA fiber embedding can be very useful in enhancing thermal stability through delaying the occurrence of thermal buckling along with decreasing the postbuckling deflection. It is also found that at low and medium sound pressure levels, the response of the SMAHC plate may not be favorable regarding fatigue-life performance, because low and medium SPLs have higher vibration amplitudes than those of the traditional composite plate. But for the composite-plate response, the low vibration amplitudes about one of the thermal buckling equilibrium positions may not be favorable regarding aerodynamic performance.

At high sound pressure levels, the SMA fiber embedding has no pronounced effect on the response, because the acoustic pressure completely dominates the thermal and constrained shape-recovery stresses.

References

[1] Tauchart, T. R., "Thermally Induced Flexure, Buckling, and Vibration of Plates," *Applied Mechanics Reviews*, Vol. 44, No. 8, Aug. 1991, pp. 347–360.

[2] Thornton, E. A., "Thermal Buckling of Plates and Shells," *Applied Mechanics Reviews*, Vol. 46, No. 10, Oct. 1993, pp. 485–506.

[3] Gray, C. C., and Mei, C., "Finite Element Analysis of Thermal Postbuckling and Vibrations of Thermally Buckled Composite Plates," *32nd AIAA/ASME/ASCE/AHS/ASC Structures, Structural Dynamics, and Materials Conference*, Pt. 4, AIAA, Washington, DC, 1991, pp. 2996–3007.

[4] Shi, Y., Lee, R. Y. Y., and Mei, C., "Thermal Postbuckling of Composite Plates Using the Finite Element Modal Coordinate Method," *Journal of Thermal Stresses*, Vol. 22, No. 6, Aug. 1999, pp. 595–614.
doi:10.1080/014957399280779

[5] Jones, R., and Mazumdar, J., "Vibration and Buckling of Plates at Elevated Temperatures," *International Journal of Solids and Structures*, Vol. 16, No. 1, 1980, pp. 61–70.
doi:10.1016/0020-7683(80)90095-5

[6] Shi, Y., Lee, R. Y., and Mei, C., "Coexiting Thermal Postbuckling of Composite Plates with Initial Imperfections Using Finite Element Modal Method," *Journal of Thermal Stresses*, Vol. 22, No. 6, 1999, pp. 595–614.
doi:10.1080/014957399280779

[7] Ibrahim, H. H., Tawfik, M., and Al-Ajmi, M., "Aero-Thermo-Mechanical Characteristics of Functionally Graded Material Panels with Temperature-Dependent Material Properties," Eighth International Congress of Fluid Dynamics and Propulsion (ICFDP 8), American Society of Mechanical Engineers Paper ICFDP-EG-116, Dec. 2006.

[8] Ibrahim, H. H., Tawfik, M., and Al-Ajmi, M., "Non-Linear Panel Flutter for Temperature-Dependent Functionally Graded Material Panels," *Computational Mechanics (online)*, Vol. 41, No. 2, 2007, pp. 325–334.
doi:10.1007/s00466-007-0188-4

[9] Ibrahim, H. H., Tawfik, M., and Al-Ajmi, M., "Thermal Buckling and Nonlinear Flutter Behavior of Functionally Graded Material Panels," *Journal of Aircraft*, Vol. 44, No. 5, 2007, pp. 1610–1618.

[10] Vaicaitis, R., "Nonlinear Response and Sonic Fatigue of National Aerospace Space Plane Surface Panels," *Journal of Aircraft*, Vol. 31, No. 1, 1994, pp. 10–18.

[11] Istenes, R. R., Rizzi, S. A., and Wolfe, H. F., "Experimental Nonlinear Random Vibration Results of Thermally Buckled Composite Panels," *36th Structures, Structural Dynamics, and Materials Conference*, AIAA, Washington, DC, Apr. 1995, pp. 1559–1568.

[12] Ng, C. F., and Clevenson, S. A., "High-Intensity Acoustic Tests of a Thermally Stressed Plate," *Journal of Aircraft*, Vol. 28, No. 4, 1991, pp. 275–281.

[13] Murphy, K. D., Virgin, L. N., and Rizzi, S. A., "Characterizing the Dynamic Response of a Thermally Loaded Acoustically Excited Plate," *Journal of Sound and Vibration*, Vol. 196, No. 5, 1996, pp. 635–658.
doi:10.1006/jsvi.1996.0506

[14] Kavallieratos, P., and Vaicaitis, R., "Nonlinear Response of Composite Panels of High Speed Aircraft," *Journal of Composite Engineering*, Vol. 3, Nos. 7–8, 1993, pp. 645–660.

[15] Locke, J. E., "Finite Element Large Deflection Random Response of Thermally Buckled Plates," *Journal of Sound and Vibration*, Vol. 160, No. 2, 1993, pp. 301–312.
doi:10.1006/jsvi.1993.1025

[16] Abdel-Motagaly, K., Duan, B., and Mie, C., "Nonlinear Response of Composite Panels Under Combined Acoustic Excitation and Aerodynamic Pressure," *AIAA Journal*, Vol. 38, No. 9, 2000, pp. 1534–1542.

[17] Dhainaut, J. M., Duan, B., Mei, C., Spottswood, S. M., and Wolfe, H. F., "Nonlinear Response of Composite Panels to Random Excitations at Elevated Temperatures," *Structural Dynamics: Recent Advances*, Southampton Univ., Southampton, England, U.K., July 2000, pp. 769–784.

[18] Dhainaut, J. M., Gou, X., and Mei, C., "Nonlinear Random Response of Panels in an Elevated Thermal-Acoustic Environment," *Journal of Aircraft*, Vol. 40, No. 4, 2003, pp. 683–691.

[19] Dhainaut, J. M., and Mei, C., "Nonlinear Response and Fatigue Life of Isotropic Panels Subjected to Non-White Noise," *Journal of Aircraft*, Vol. 43, No. 4, 2006, pp. 975–979.

[20] Ibrahim, H. H., Tawfik, M., and Al-Ajmi, M., "Random Response of Functionally Graded Material Panels Subject to White-Gaussian Noise and Thermal Environment," *12th International Conference on Aerospace Sciences and Aviation Technology* [CD-ROM], Military Technical College, Cairo, Egypt, 29–31 May 2007.

[21] Cross, W. B., Kariotis, A. H., and Stimeler, F. J., "Nitinol Characterization Study," NASA CR-14B, 1969.
[22] Birman, V., "Review of Mechanics of Shape Memory Alloy Structures," *Applied Mechanics Reviews*, Vol. 50, No. 11, 1997, pp. 629–645.
[23] Jia, J., and Rogers, C. A., "Formulation of a Mechanical Model for Composites with Embedded SMA Actuators," *Journal of Mechanical Design*, Vol. 114, 1992, pp. 670–676.
[24] Tawfik, M., Ro, J. J., and Mei, C., "Thermal Postbuckling and Aeroelastic Behavior of Shape Memory Alloy Reinforced Plates," *Smart Materials and Structures*, Vol. 11, No. 2, 2002, pp. 297–307. doi:10.1088/0964-1726/11/2/313
[25] Park, J. S., Kim, J. H., and Moon, S. H., "Vibration of Thermally Post-Buckled Composite Plates Embedded with Shape Memory Alloy Fibers," *Composite Structures*, Vol. 63, No. 2, 2004, pp. 179–188. doi:10.1016/S0263-8223(03)00146-6
[26] Gilat, R., and Aboudi, J., "Dynamic Response of Active Composite Plates: Shape Memory Alloy Fibers in Polymeric/Metallic Matrices," *International Journal of Solids and Structures*, Vol. 41, No. 20, 2004, pp. 5717–5731. doi:10.1016/j.ijsolstr.2004.04.043
[27] Guo, X., Przckop, A., and Mei, C., "Reduction of Random Response of Composite Plates Using Shape Memory Alloy in Thermal Environments," 45th AIAA/ASME/ASCE/ AHS/ASC Structures, Structural Dynamics, and Materials Conference, Palm Springs, CA, AIAA Paper 2004-1635, 2004.
[28] Ibrahim, H. H., Tawfik, M., and Negm, H. M., "Thermal Postbuckling and Flutter Behavior of Shape Memory Alloy Hybrid Composite Plates," Eighth International Congress of Fluid Dynamics and Propulsion (ICFDP 8), American Society of Mechanical Engineers Paper ICFDP-EG-153, Dec. 2006.
[29] Reddy, J. N., Theory and Analysis of Elastic Plates, Taylor and Francis, Philadelphia, 1999.
[30] Xue, D. Y., "Finite Element Frequency Domain Solution of Nonlinear Panel Flutter with Temperature Effects and Fatigue Life Analysis," Ph.D. Dissertation, Mechanical Engineering Dept., Old Dominion Univ., Norfolk, VA, 1991.
[31] Bathe, K. J., *Finite Element Procedures*, Prentice–Hall, Englewood Cliffs, NJ, 1996.